

See discussions, stats, and author profiles for this publication at: <https://www.researchgate.net/publication/272102141>

Global analysis of peroxy radicals and peroxy radical–water complexation using the STOCHEM–CRI global chemistry and transport model

ARTICLE *in* ATMOSPHERIC ENVIRONMENT · APRIL 2015

Impact Factor: 3.28 · DOI: 10.1016/j.atmosenv.2015.02.020

CITATION

1

READS

32

12 AUTHORS, INCLUDING:



[Anwar H Khan](#)

University of Bristol

29 PUBLICATIONS 135 CITATIONS

[SEE PROFILE](#)



[S. R. Utembe](#)

University of Melbourne

38 PUBLICATIONS 705 CITATIONS

[SEE PROFILE](#)



[Alexander Thomas Archibald](#)

University of Cambridge

45 PUBLICATIONS 404 CITATIONS

[SEE PROFILE](#)

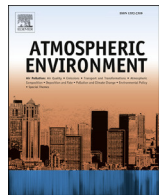


[Dudley E. Shallcross](#)

University of Bristol

239 PUBLICATIONS 3,509 CITATIONS

[SEE PROFILE](#)



Global analysis of peroxy radicals and peroxy radical-water complexation using the STOCHEM-CRI global chemistry and transport model



M.A.H. Khan ^a, M.C. Cooke ^{a,1}, S.R. Utembe ^{a,2}, A.T. Archibald ^{a,3}, R.G. Derwent ^b, M.E. Jenkin ^c, W.C. Morris ^a, N. South ^a, J.C. Hansen ^d, J.S. Francisco ^e, C.J. Percival ^f, D.E. Shallcross ^{a,*}

^a Biogeochemistry Research Centre, School of Chemistry, University of Bristol, Cantock's Close, Bristol BS8 1TS, UK

^b rdsscientific, Newbury, Berkshire, UK

^c Atmospheric Chemistry Services, Okehampton, Devon EX20 4QB, UK

^d Department of Chemistry and Biochemistry, Brigham Young University, Provo, UT 84602, USA

^e Department of Earth Atmospheric Planetary Sciences, Purdue University, West Lafayette, IN 47907-2051, USA

^f The Centre for Atmospheric Science, The School of Earth, Atmospheric and Environmental Science, The University of Manchester, Simon Building, Brunswick Street, Manchester M13 9PL, UK

HIGHLIGHTS

- RO₂-H₂O complexes are postulated to perturb RO₂ chemistry.
- The presence of RO₂-H₂O complexes has been found substantially in tropics.
- RO₂-H₂O complexation appears to play a significant role in the upper troposphere.

ARTICLE INFO

Article history:

Received 22 July 2014

Received in revised form

5 February 2015

Accepted 6 February 2015

Available online 7 February 2015

Keywords:

Peroxy radical

Peroxy radical-water complexation

STOCHEM-CRI

Global sources

Global sinks

ABSTRACT

The importance of peroxy radical (RO₂) chemistry in the troposphere is investigated using the STOCHEM-CRI global chemistry and transport model. The oxidation of VOCs leads to the formation of RO₂ radicals which are dominated by CH₃O₂ (83%), RCO₃ (5%), isoprene derived peroxy radicals (6%), and terpene derived peroxy radicals (1%). A good correlation between model and field measurements for total RO₂ for most of the selected stations suggests that they are appropriate background sites as the atmospheric processes occurring at these stations are representative of the chemistry taking place within the entire model grid square in which they are located. The seasonality exhibited by RO₂ has been studied, with well-defined cycles (highest in summer and lowest in winter) seen in both hemispheres. Peroxy radical-water complexes, whilst not represented using Chemical Transport Models (CTMs) previously, are postulated to perturb RO₂ chemistry. The significance of water clusters (RO₂-H₂O) is investigated using the STOCHEM-CRI model and reveals that at 300 K the proportion of RO₂ participating in complexation with water is approximately 12% in the tropics. Isoprene derived radicals are the most strongly bound of RO₂ species investigated and their degree of complexation at approx. 300 K far surpasses that of the generic peroxy radicals by 3–5%. At higher altitudes (approx. 8 km) characterized by sub-ambient temperatures, the fraction of RO₂-H₂O complex that can exist is approximately 17% in the upper troposphere above Mace Head (Northern Hemisphere), 14% above Cape Grim (Southern Hemisphere), and 8% above Mauna Loa (Tropics).

© 2015 The Authors. Published by Elsevier Ltd. This is an open access article under the CC BY license (<http://creativecommons.org/licenses/by/4.0/>).

* Corresponding author.

E-mail address: d.e.shallcross@bristol.ac.uk (D.E. Shallcross).

¹ Now at the Met Office, FitzRoy Road, Exeter, Devon EX1 3PB, UK.

² Now at the School of Earth Sciences, University of Melbourne, Parkville, VIC 3010, Australia.

³ Now at the NCAS- Climate and the Centre for Atmospheric Science, University of Cambridge, Cambridge, UK.

1. Introduction

Alkyl peroxy radicals (RO₂) are short lived species generated from the oxidation of volatile organic compounds (VOCs) by OH, NO₃, Cl, and O₃. They are important reactive intermediates/chain

propagation species which affect the lifetime of trace gases through their impact on OH (Heard and Pilling, 2003; Monks, 2005). In the troposphere, RO₂ radicals can participate in several gas phase reactions depending on the regime in which they are present. Traditionally, the literature has referred to two such regimes; the low NO_x regime – where the fate of RO₂ is dominated by reactions other than that with NO; and the high NO_x regime – where the fate of RO₂ is dominated by their reaction with NO. In the polluted environment, the oxidation of NO by RO₂ leads to NO₂ formation and subsequently ozone formation in the troposphere (e.g. Lightfoot et al., 1992; Jenkin and Clemishaw, 2000; Burkert et al., 2001). However, under conditions where the concentration of NO_x is low enough that the reaction between RO₂ and NO does not account for the major loss of RO₂ ([NO] ~ 1–10 pptv), one of the dominant fates of RO₂ is either self-reaction or cross-reaction with other peroxy radicals (Lightfoot et al., 1992; Wallington et al., 1992; Tyndall et al., 2001; Madronich and Calvert, 1990). A knowledge of peroxy radical abundances and distributions is essential to determine the oxidising capacity of the lower atmosphere in general (Thompson, 1992) and to determine oxidation rates and hence transformations of primary pollutants on a variety of scales. In spite of their importance in the chemical processing of the troposphere, there are few measurement data available (Cantrell et al., 1992, 1996; Carpenter et al., 1997; Zanis et al., 1999; Burkert et al., 2001, 2003; Hanke et al., 2002; Handisides et al., 2003; Mihelcic et al., 2003; Green et al., 2003; Fleming et al., 2006a, 2006b; Kukui et al., 2008; Liu et al., 2009; Andres-Hernandez et al., 2001, 2009). The reported abundances of peroxy radicals during different field studies have large variability and apart from Electron Spin Resonance (ESR) type studies (e.g. Fuchs et al., 2009) report total RO₂ where it is possible for there to be different contributions to the total RO₂ signals. The most common measurement technique, PERCA (Peroxy radicals by chemical amplification; Cantrell et al., 1984), operates by inferring the RO₂ abundance based on measuring the chain length of NO–NO₂ conversions. PERCA requires detailed calibration procedures and it is well known that different peroxy radicals will generate different chain lengths, leading to unavoidable uncertainty. However, given our mechanistic understanding of the role of RO₂ in tropospheric photochemistry, it is conceivable that the results from photochemical models should give a reasonably accurate dataset and the comparison of model prediction with measurements will improve the understanding of atmospheric chemical mechanisms. The global budget and the global distribution of RO₂ have been presented in this modelling study using the STOCHEM-CRI global 3-dimensional chemistry transport model.

Aloisio and Francisco (1998) postulated that a significant proportion of RO₂ could exist in water-complexed forms in the marine boundary layer and in the tropical troposphere which were overlooked or not detected by instruments (e.g. PERCA). Although the HO₂.H₂O term has been included as an additional term for the calculation of the HO₂ + HO₂ termination step (Sander et al., 2011), the water influence on the abundances of RO₂ throughout the troposphere has, up to now, been ignored in many atmospheric modelling studies. The energetics and potential impacts of hydroperoxyl radical-water complexes (HO₂.H₂O) and organic peroxy radical-water complexes (RO₂.H₂O) were presented in previous theoretical chemistry studies (Aloisio and Francisco, 1998; Clark et al., 2008, 2010; Archibald et al., 2011) by calculating the optimal geometries, binding energies, and equilibrium constants of the respective complexes. Experimental observations of HO₂.H₂O and RO₂.H₂O complexes are quite difficult, but, HO₂.H₂O complexation was observed by different infrared spectroscopic techniques (Aloisio et al., 2000; Kanno et al., 2006). The estimation by Aloisio and Francisco (1998) showed that 29% of all HO₂ radicals

present in the atmosphere could participate in water complexation under ambient conditions. Clark et al. (2008) demonstrated that at tropospheric temperatures it is possible for RO₂.H₂O complexes with sufficient binding energies to exist in the troposphere (e.g. CH₃O₂.H₂O complex with 2.3 kcal/mol and CH₂(OH)O₂.H₂O complex with 5.1 kcal/mol). The species having largest binding energies (>5 kcal/mol) are most likely to play important chemical roles under low-temperature conditions (Clark et al., 2008). In this study, the abundances of RO₂.H₂O are calculated over a range of relative humidity and temperature from the data output by the STOCHEM-CRI. Using equation (1) the ratio between complexed and uncomplexed RO₂ are determined.

$$K_{eq}*[H_2O] = [RO_2.H_2O]/[RO_2] \quad (1)$$

The equilibrium constant, K_{eq} taken from the literature (Clark et al., 2008, 2010) is used to calculate the RO₂.H₂O concentration. Aloisio and Francisco (1998) suggested that the RO₂.H₂O complexes could exist in significant abundance in the lower region of the atmosphere where conditions of high water density and low temperature could favour its formation. The equilibrium constant for peroxy radical–water complex formation decreases with increasing temperature, but is also dependent on water vapour levels, so it is not entirely straightforward predicting where elevated levels of complex may reside. For example at the surface, in the tropics the water concentration is high but so is temperature, whereas in high latitudes it is cold but often very dry. So the understanding of the implications of the abundances and distribution of RO₂.H₂O complexes is necessary because of their possible important role in troposphere. In this study, the global distribution of these RO₂.H₂O complexes is studied using the STOCHEM-CRI model.

2. Experimental

2.1. Global chemistry transport model studies

The global chemistry transport model, STOCHEM used in this study, is a 3-D model that has widely been used in studies of tropospheric chemistry and subsequently enables advanced spatial resolution of tropospheric pollution. The model transports a myriad of chemical species that are subject to chemical reactions and physical processes. It takes a Langrangian approach with respect to transport as all species are advected in unison. The chemistry and transport processes are subsequently uncoupled enabling local determination of the timestep. Lagrangian cells are advected according to winds taken from the Meteorological Office Unified Model archive which stores 6-hourly wind, temperature, specific humidity, tropopause height and boundary layer depth data on a 1.25° longitude × 0.83° latitude grid. The STOCHEM model has an associated advection timestep of 5 min which is sufficient to monitor the chemical evolution of each of the 50,000 Lagrangian air parcels but short enough to maintain numerical stability. An initial description of the model was given by Collins et al. (1997) and an updated report was detailed by Utembe et al. (2009). This particular version of the model is described by Derwent et al. (2008) with an organic aerosol module and a more extensive chemical scheme introduced by Utembe et al. (2010, 2011). The chemical mechanism used in STOCHEM, is the common representative intermediates mechanism version 2 and reduction 5 (CRI v2-R5), referred to as 'STOCHEM-CRI'. The detail of the CRI v2-R5 mechanism is given by Jenkin et al. (2008), Watson et al. (2008), and Utembe et al. (2009) with updates highlighted in Utembe et al. (2010). The mechanism describes the oxidation of 27 emitted VOCs and consists of 229 chemical species taking part in 627 chemical and photochemical

Table 1

Main sources and sinks of the selected RO₂ radicals. Values are given as a percentage of the global production and loss of RO₂.

Sources	Global contribution (%)	Sinks	Global contribution (%)
CH₃O₂			
OH + CH ₄ → CH ₃ O ₂	52.9	CH ₃ O ₂ + NO → HCHO + HO ₂ + NO ₂	48.5
OH + CH ₃ OOH → CH ₃ O ₂	28.3	CH ₃ O ₂ + HO ₂ → CH ₃ COOH	45.2
CH₃CO₃			
OH + CH ₃ CO ₃ H → CH ₃ CO ₃	21.9	CH ₃ CO ₃ + NO → CH ₃ O ₂ + NO ₂	53.2
OH + CH ₃ CHO → CH ₃ CO ₃	13.9	CH ₃ CO ₃ + HO ₂ → CH ₃ CO ₃ H	28.3
CARB6 → CH ₃ CO ₃ + CO + HO ₂	9.9	CH ₃ CO ₃ → CH ₃ O ₂	17.4
RU12O2 + NO → CH ₃ CO ₃ + HOCH ₂ CHO + NO ₂	9.4		
RU10O2 + NO → CH ₃ CO ₃ + HOCH ₂ CHO + NO ₂	7.7		
OH + CARB6 → CH ₃ CO ₃ + CO	6.4		
RU14O2			
OH + C ₅ H ₈ → RU14O2	100.0	RU14O2 + NO → UCARB10 + HCHO + HO ₂ + NO ₂	35.7
		RU14O2 + HO ₂ → RU14OOH	40.8
RU12O2			
OH + UCARB12 → RU12O2	46.2	RU12O2 + HO ₂ → RU12OOH	46.4
OH + RU12OOH → RU12O2	43.7	RU12O2 + NO → CH ₃ CO ₃ + HOCH ₂ CHO + NO ₂	23.9
RU10O2			
OH + UCARB10 → RU10O2	48.1	RU10O2 + HO ₂ → RU10OOH	40.8
OH + RU10OOH → RU10O2	41.4	RU10O2 + NO → CH ₃ CO ₃ + HOCH ₂ CHO + NO ₂	35.7
NRU14O2			
NO ₃ + C ₅ H ₈ → NRU14O2	100	NRU14O2 → NUCARB12 + HO ₂	42.7
		NRU14O2 + HO ₂ → NRU14OOH	35.3
RTN28O2			
OH + α-pinene → RTN28O2	100	RTN28O2 + NO → TNCARB26 + HO ₂ + NO ₂	43.9
		RTN28O2 + HO ₂ → RTN28OOH	36.6
		RTN28O2 + NO → RTN28NO ₃	14.6
NRTN28O2			
NO ₃ + α-pinene → NRTN28O2	100	NRTN28O2 + HO ₂ → NRTN28OOH	42.0
OH + NRTN28OOH → NRTN28O2	46.1	NRTN28O2 + NO → TNCARB26 + NO ₂	39.1
RTX28O2			
OH + β-pinene → RTX28O2	60	RTX28O2 + HO ₂ → RTX28OOH	44.2
OH + RTXOOH → RTX28O2	40	RTX28O2 + NO → TXCARB24 + HCHO + HO ₂ + NO ₂	35.8
		RTX28O2 + NO → RTX28NO ₃	11.9
NRTX28O2			
NO ₃ + β-pinene → NRTX28O2	53.9	NRTX28O2 + HO ₂ → NRTX28OOH	55.3
OH + NRTX28OOH → NRTX28O2	46.1	NRTX28O2 + NO → TXCARB24 + HCHO + NO ₂	36.1

Notes: Identities of the peroxy radicals can be found in Appendix B. Closest MCM analogues of CARB6, UCARB10, UCARB12, TNCARB26, and TXCARB24 are MGLYOX, MVK/MACR, HC4CCHO, PINAL, and NOPINONE, respectively. Structures of the species in the reaction can be obtained using species name and search facility on MCM website (<http://mcm.leeds.ac.uk/MCM/search.htm>).

reactions. The emission data used in STOCHEM model were adapted from the Precursor of Ozone and their Effects in the Troposphere (POET) inventory (Granier et al., 2005) for the year 1998 (more detailed emissions data can be found in Appendix A).

STOCHEM output is provided on a 5° × 5° grid which corresponds to an average occupancy of approximately two air parcels per square. The output is consequently a coarse-scale average over urban, rural, and remote location; thus inaccuracies can arise when comparing the model output with field measurements. Additionally, when the number of parcels is limited interpolation errors can arise in circumstances where grid squares do not contain any Lagrangian cells. STOCHEM has previously been used for global investigations, including those modelling the transport of chemical species (Collins et al., 1999; Johnson et al., 2002; Sanderson et al., 2003). In this study, STOCHEM is used to reveal the global burden of peroxy radicals, their localised concentrations at specific measurement stations, and the distribution of RO₂-H₂O complexes. The simulation was conducted with meteorology from 1998 for a period of 24 months with the first 12 allowing the model to spin up. Analysis is performed on the subsequent 12 months of data.

3. Results and discussion

3.1. Peroxy radical

The complexity in the oxidation of the 16 originally emitted VOCs in STOCHEM-CRI leads to the production of 47 organic peroxy

radical species which leads to an increase in overall RO₂ concentration compared with the original STOCHEM model (Cooke, 2010). In our model studies, the dominant RO₂ species are found to be CH₃O₂ (83%) followed by isoprene peroxy radicals (RU14O2, RU12O2, RU10O2, and NRU14O2) (6%), RCO₃ (5%), and terpene peroxy radicals (NRTN28O2, NRTX28O2, RTN28O2, RTX28O2) (1%) (see Appendix B for identities). Peroxy radical formation is dominated by the reactions of OH with VOCs, and regeneration from the reaction of OH with the organic hydroperoxide reservoir species, ROOH. Consistent with a number of other modelling studies, we find that the reaction of RO₂ with NO and HO₂ are the main atmospheric sinks of RO₂. Peroxy radical cross reactions act as another non-negligible loss process. Table 1 shows the contribution of the sources and sinks (in percentage) to the global fluxes of some dominating peroxy radicals. CH₃O₂ is predominantly derived from CH₄ (53%). The remaining sources originate from CH₃OOH (28%) with the balance from the oxidation of larger VOCs. RCO₃ is formed from the degradation of many VOCs (e.g. aldehydes) in the model. Isoprene undergoes oxidation via OH or O₃ during the daytime and via NO₃ at nighttime to form isoprene peroxy radicals. The terpene derived peroxy radicals originate specifically from the oxidation of α-pinene and β-pinene, which are used to represent all terpene emissions.

RO₂ is predominantly derived from the oxidation of VOCs, so the peak [RO₂] (between 30 pptv and 40 pptv) is found in the surface layer located over areas with large VOC emissions, high unwavering temperature levels and photolysis rates (e.g. the tropics, see Fig. 1a).

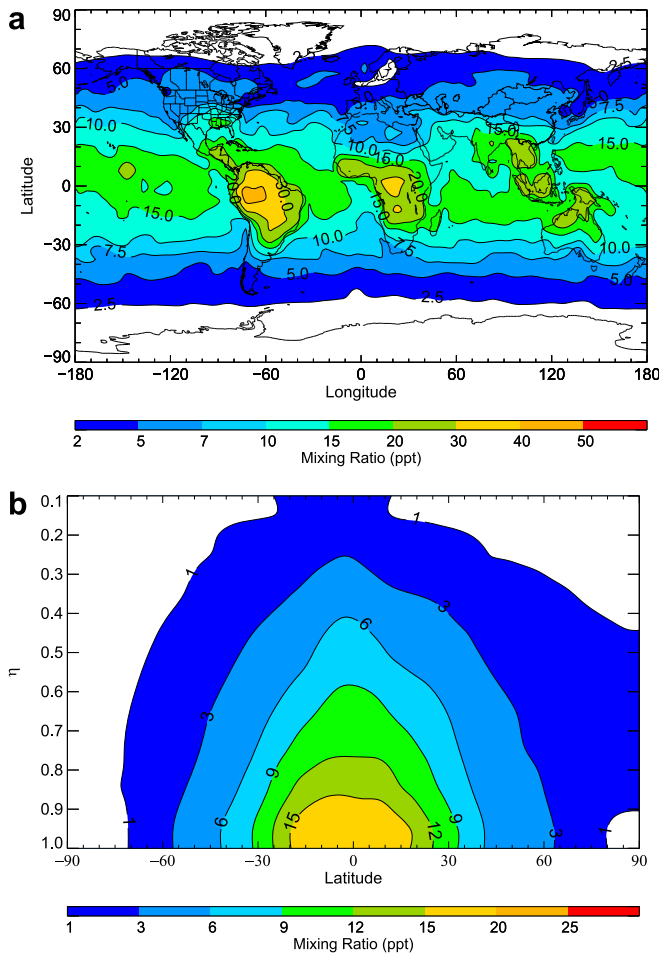


Fig. 1. (a) Annual mean surface level distribution of RO₂ simulated by the STOCHEM-CRI, (b) Annual mean zonal average distribution of RO₂ simulated by the STOCHEM-CRI.

The zonal distribution shows a peak at the surface around the equator where there are large emissions of VOCs from forested areas and high levels of photochemical activity. The RO₂ abundances are found to decrease with altitude (Fig. 1b).

The twelve surface measurement campaigns selected for analysis are shown in Table 2. The seasonal variation of the peroxy radical surface concentration of the stations situated in the Northern hemisphere showed that RO₂ abundances are at their highest during the summer months, reaching maximum levels in

July and August (Fig. 2). During summer, O₃ photolysis is at its highest and the humidity is increased, so the photolytic reactions involving the resultant OH radical lead to the formation of high concentrations of RO₂. Minimum values are seen during the winter months, typically in December and January when the solar intensity is diminished. Data obtained from the Southern hemisphere station, Cape Grim, demonstrates an opposite but analogous seasonal trend. Maximum and minimum values are recorded in June and January, respectively (Fig. 2).

The modelled data were monthly averages for the year 1998 which were compared with the selected field measurement data recorded in the equivalent months of their respective campaign years. Most of the measurement data were published as a combination of both HO₂ and RO₂, so we calculated the concentrations of HO₂ + RO₂ from STOCHEM-CRI and then compared them with the measured HO₂ + RO₂ data (Fig. 2). In general, the field campaigns yield higher peroxy radical concentrations than the model, which is not surprising given that the model contains only a limited number of the peroxy radical precursors (VOCs).

The deviation between the monthly mean model and the respective monthly measurement data are small for most of the stations (e.g. Mace Head, Weybourne, Jungfraujoch, Pabstthum, Idaho Hill, Rishiri Island, and Mauna Loa). The greatest deviations from model values occur at Alabama, Sacramento, Hohenpeissenberg, and Sable Island, and may result from unexpected meteorological events, the presence of biomass burning plumes or periods of intense solar insulation. The model is driven by the meteorology of year 1998 and the global surface emissions of CO, NO_x, and NMVOCs for the year of 1998 were used in the model. But most of the field measurement data were recorded during years other than 1998, which subsequently complicates their comparison with the modelled data. The low resolution of our model, which computes average concentrations over each grid square of dimensions 5° latitude × 5° longitude will also tend to lead to an under-prediction by the model. The measurement data for Hohenpeissenberg is found to be 5-fold higher than the model results. The Hohenpeissenberg station is located in a rural agricultural and forested area; the air arriving at this measurement site due to convective lifting of the boundary layer is enriched in a number of biogenic VOCs (e.g. terpenes and isoprene) with surface sources. The polluted air masses from the East of Hohenpeissenberg (Kaiser et al., 2007) contribute additional VOC, leading to overall higher production of RO₂. The duration of the field campaigns varies from day to night and days to months, which causes variation between the model and measurement data if there is a local source around the monitoring station. The results of the field studies conducted at Cape Grim during February deviate from the expected trend as they are 4-fold lower than those output from the model because in our model Tasmania sits in the same grid square as Melbourne and is therefore

Table 2

Details of the respective locations analysed in the model study, their associated field campaign and the year in which they were conducted.

Location	Latitude	Longitude	Year	Measurement type	Field campaign	Source
Pabstthum	53°N	13°E	1998	MIESR	BERLIOZ	Geyer et al., 2003
Weybourne	53°N	1°E	2002	PERCA	WAOWEX, INSPECTRO	Fleming et al., 2006a
Mace Head	53°N	10°W	2002	PERCA	NAMBLEX	Fleming et al., 2006b
Hohenpeissenberg	48°N	11°E	2000	IMG-CA	HOPE	Handsides et al., 2003
Jungfraujoch	46°N	8°E	1996	PERCA	FREETEX	Zanis et al., 1999
Rishiri Island	45°N	141°E	2003	PERCA	RISFEX	Bin et al., 2009
Idaho Hill	40°N	105°W	2003	PERCA	TOHPE	Cantrell et al., 1997
Mauna Loa	19°N	155°W	1992	PERCA	MIOPLEX	Cantrell et al., 1996
Cape Grim	41°S	145°E	1995	PERCA	SOAPEX	Monks et al., 1998
Sable Island	44°N	60°W	1993	PERCA	NARE	Duderstadt et al., 1998
Sacramento	39°N	120°W	2007	TD-CIMS	BEARPEX	LaFranchi et al., 2009
Alabama	32°N	88°W	1990	PERCA	ROSE	Cantrell et al., 1993

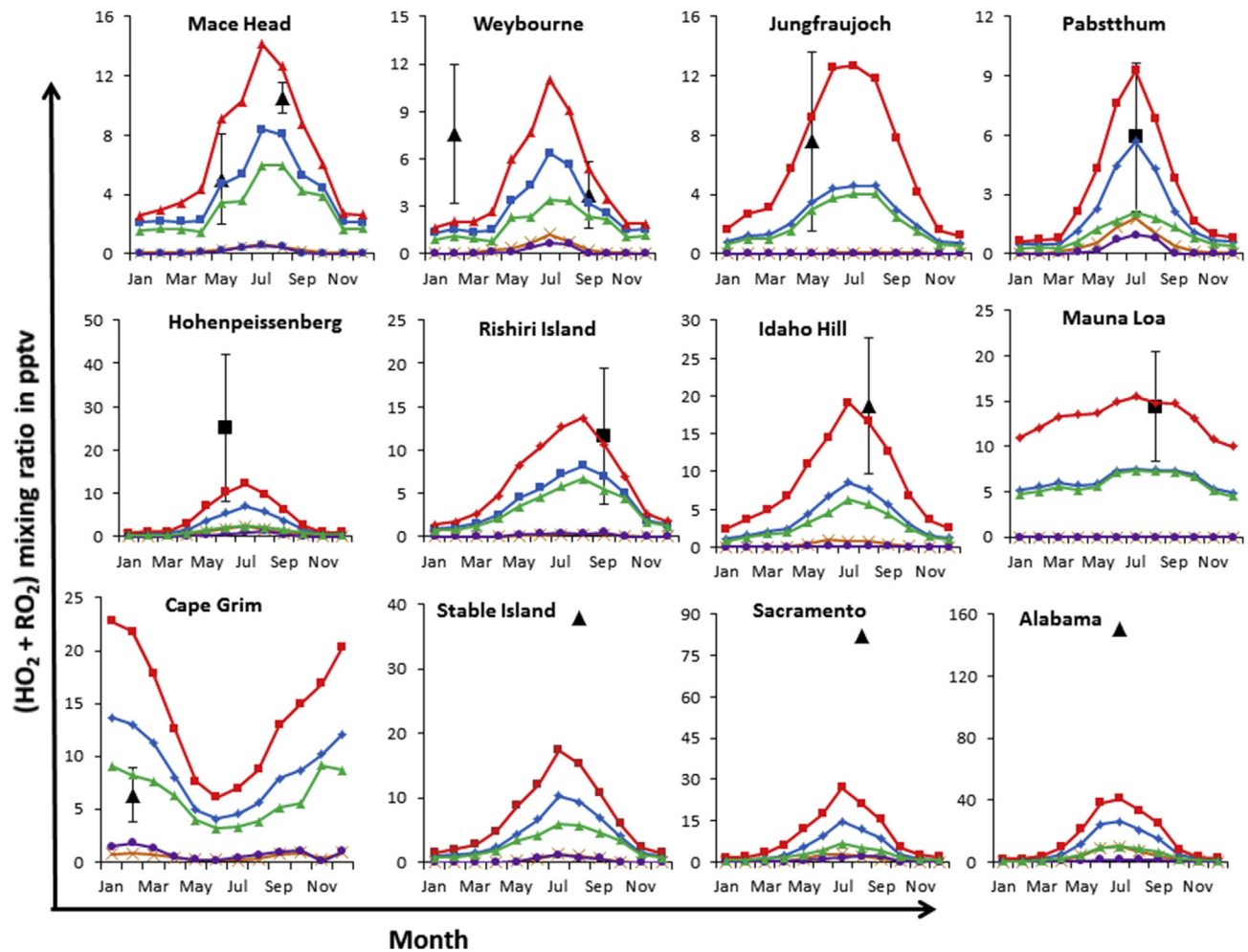


Fig. 2. Monthly variation of surface global RO_2 and $\text{RO}_2 + \text{HO}_2$ abundances of selected monitoring stations produced by the STOCHEM-CRI, the blue line represents RO_2 , red line represents $\text{RO}_2 + \text{HO}_2$, green line represents CH_3O_2 , yellow line represents isoprene derived peroxy radicals, violet line represents terpene derived peroxy radicals, black square symbols represent the measurement data of RO_2 and black triangle symbols represent the measurement data of $\text{RO}_2 + \text{HO}_2$. (For interpretation of the references to colour in this figure legend, the reader is referred to the web version of this article.)

representative of the chemistry taking place within the entire grid square in which Cape Grim is located. The Mauna Loa Observatory is located on the Island of Hawaii at an elevation of 3397 m and situated in the tropics where both sunlight and temperature are not changing significantly with seasonal changes, so the changes in peroxy radical levels throughout the progression of the seasons consist of a series of non-descript peaks and troughs. However, the peak through June to September has been found because of an increase in OH (due to higher solar intensity) resulting in higher abundances of peroxy radicals. Mauna Loa is affected by long-range transport from Asia during spring (Jaffe et al., 1997), which may be responsible for the small peak in March in our model data.

3.2. Peroxy radical-water complexes

Clark et al. (2008) showed the potential importance of organic peroxy radical-water complexes because of the positive relationship of the binding energies of the complexes and their associated equilibrium constants. Different $\text{RO}_2\text{H}_2\text{O}$ complexes exhibit variable binding energies (e.g. weakest for $\text{CH}_3\text{O}_2\text{H}_2\text{O}$ and strongest for $\text{OHCH}_2\text{O}_2\text{H}_2\text{O}$). A significant fraction (10–25%) of RO_2 can exist as $\text{RO}_2\text{H}_2\text{O}$ complex (Clark et al., 2008) for the species with strong binding energies (~5–7 kcal/mol). Utilization of the equilibrium

constant ($1.54 \times 10^{-21} \text{ cm}^3 \text{ molecule}^{-1}$ for $\text{CH}_3\text{O}_2\text{H}_2\text{O}$) from Clark et al. (2008) gives a lower limit for peroxy radical complexation, suggesting that at 300 K, no more than 0.1% of the total peroxy radical concentration participates in the formation of $\text{RO}_2\text{H}_2\text{O}$ complexes (Fig. 3). Using the equilibrium constant ($1.91 \times 10^{-19} \text{ cm}^3 \text{ molecule}^{-1}$ for $\text{OHCH}_2\text{O}_2\text{H}_2\text{O}$) from Clark et al. (2008), a considerable proportion (up to 12%) of peroxy radicals in the tropics are found to be in the form of $\text{RO}_2\text{H}_2\text{O}$ at 300 K (Fig. 4). Water vapour is the dominant variable involved in determining the proportion of RO_2 as $\text{RO}_2\text{H}_2\text{O}$. The relative abundance of the $\text{RO}_2\text{H}_2\text{O}$ complexes increases relative to the uncomplexed RO_2 radical as the abundance of atmospheric moisture is increased with increasing temperature in the tropics. Given the large sources of uncertainty associated in the determination of the binding energy of the complexes, the error associated with the model calculation of $\text{RO}_2\text{H}_2\text{O}$ abundances is of the order of a factor of at least 2, but, such an analysis highlights the potential for $\text{RO}_2\text{H}_2\text{O}$ complexation in the atmosphere and indicates which regions are affected most.

The seasonal cycle of the $\text{RO}_2\text{H}_2\text{O}$ mixing ratio is a direct result of extremes in water vapour variation throughout the year. Fig. 5 shows the annual variability in $\text{RO}_2\text{H}_2\text{O}$ at selected stations where $\text{RO}_2\text{H}_2\text{O}$ levels as a fraction of the total RO_2 concentration reach maximum in August for NH stations and in January for SH

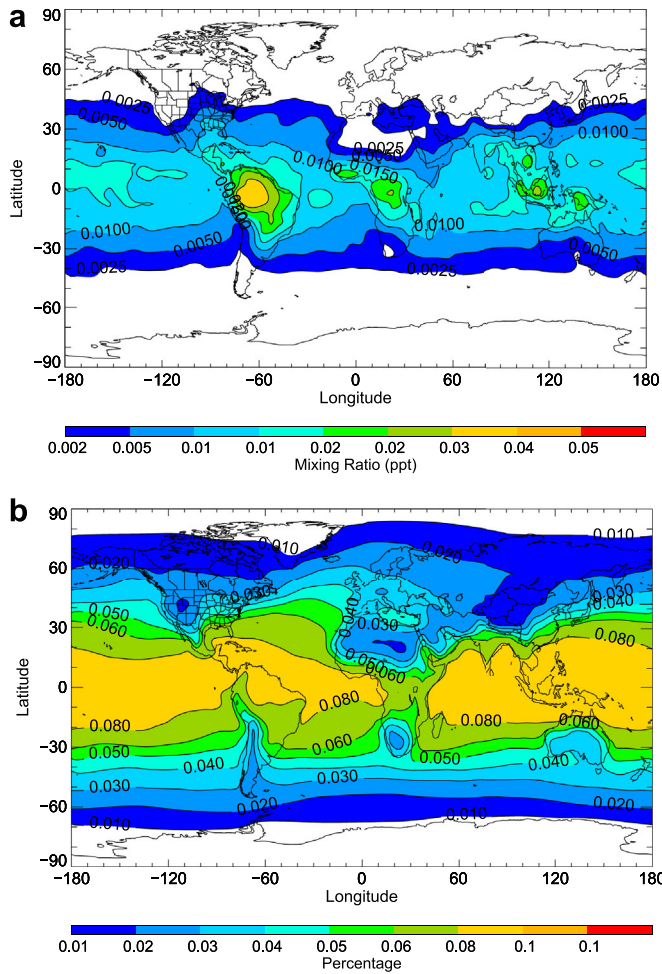


Fig. 3. Annual mean surface level distribution of all 47 $\text{RO}_2\text{H}_2\text{O}$ complexes (using a lower limit for the equilibrium constant of $1.54 \times 10^{-21} \text{ cm}^3 \text{ molecule}^{-1}$) for the year 1998 simulated by the STOCHEM-CRI, (a) mixing ratio of $\text{RO}_2\text{H}_2\text{O}$, (b) percentage of all 47 $\text{RO}_2\text{H}_2\text{O}$ complex formation with respect to total RO_2 .

station. Atmospheric moisture is highest in the summer time and therefore, water vapour abundance and temperature, exerts a larger influence on the extent of peroxy radical-water complexation. The Tropical region, such as Mauna Loa characterized by a high relative humidity, exhibits the highest levels of complexation, as shown in Fig. 5. $\text{RO}_2\text{H}_2\text{O}$ levels at Cape Grim reach a maximum of 7% in summer time (December-January-February) with a lowest of 4% in winter months (June-July-August). It is an attribute of Cape Grim thought to be due to the arrival of storms originating from the west (Southern Ocean) (Jimi et al., 2007) which inject high concentrations of water vapour into the troposphere.

Further work conducted by Clark et al. (2010) attributed significant focus on isoprene peroxy radical-water complexes, proposing geometries, lifetimes, and equilibrium constants for 8 β -hydroxy isoprene derivatives that can exist in their complexed form. The proportion of isoprene derived peroxy radicals (RU14O₂, RU12O₂, RU10O₂, and NRU14O₂) involved in the complexation has been determined at 298 K in this study. The equilibrium constant of $2.60 \times 10^{-19} \text{ cm}^3 \text{ molecule}^{-1}$, associated with the most strongly bound species the trans-4-OH isoprene hydroxyalkyl peroxy radical, was considered in the calculation in order to derive an upper complexation limit. The mixing ratio of isoprene derived $\text{RO}_2\text{H}_2\text{O}$ complexes is found to be up to 2 ppt in the tropical region. The proportion of isoprene derived peroxy radical complexed with

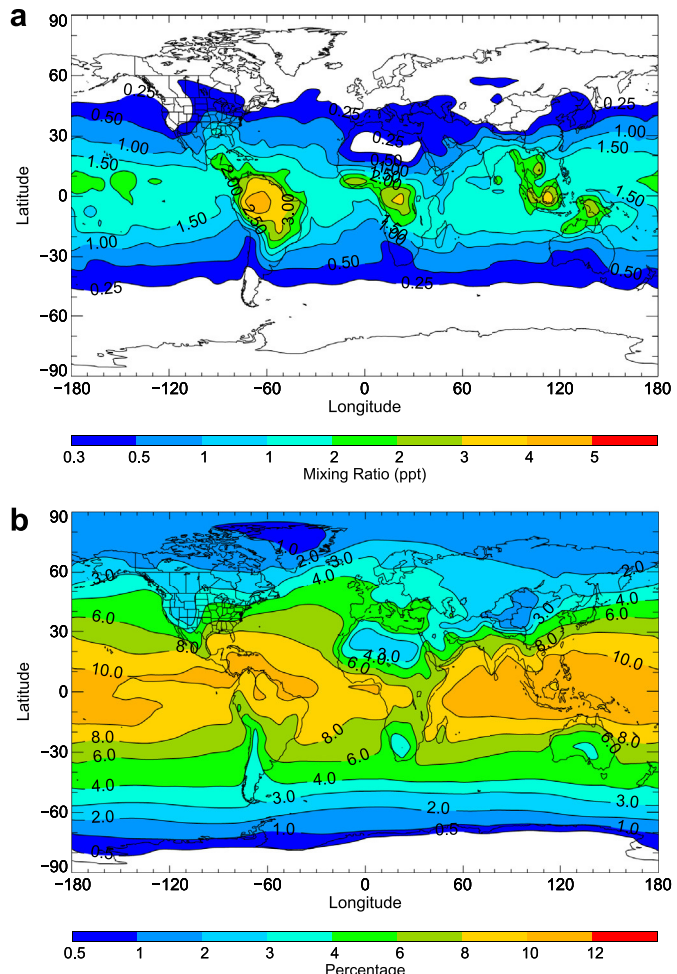


Fig. 4. Annual mean surface level distribution of all 47 $\text{RO}_2\text{H}_2\text{O}$ complexes (using an upper limit for the equilibrium constant of $1.91 \times 10^{-19} \text{ cm}^3 \text{ molecule}^{-1}$) for the year 1998 simulated by the STOCHEM-CRI, (a) mixing ratio of $\text{RO}_2\text{H}_2\text{O}$, (b) percentage of all 47 $\text{RO}_2\text{H}_2\text{O}$ complex formation with respect to total RO_2 .

water is found to be up to 15% in the tropics (Fig. 6), which is approximately 3–5% higher than the upper limit of total $\text{RO}_2\text{H}_2\text{O}$ complexation. These elevated levels suggest that radicals originating from isoprene have a particularly high affinity for water complexation.

If we use the equilibrium constant for $\text{OHCH}_2\text{O}_2\text{H}_2\text{O}$ at 200 K for the calculation of the $\text{RO}_2\text{H}_2\text{O}$ complexation at the upper troposphere (Level 9 of the model, ~14 km), where the average temperature is close to 200 K, more than 50% of RO_2 can exist complexed with H_2O . Thus, the regions of the troposphere characterized by lower temperatures, such as the upper troposphere, substantial perturbation of peroxy radical abundance and chemistry may occur.

Using the equilibrium constants for $\text{OHCH}_2\text{O}_2\text{H}_2\text{O}$ at 200 K and 300 K from Clark et al. (2008), the following exponential relationship between equilibrium constant (K_{eq}) and temperature (T) is found for $\text{RO}_2\text{H}_2\text{O}$ complexes.

$$K_{\text{eq}} = 6.692 \times 10^{-9} \exp^{-0.0809T} \quad (2)$$

Using Eq (2), the surface distribution of the $\text{RO}_2\text{H}_2\text{O}$ showed a higher mixing ratio of $\text{RO}_2\text{H}_2\text{O}$ (up to 6 ppt) in the tropics (Fig. 7a), but the percent formation of $\text{RO}_2\text{H}_2\text{O}$ with respect to RO_2 results showed higher complexation over remote oceans (up to 25%) and

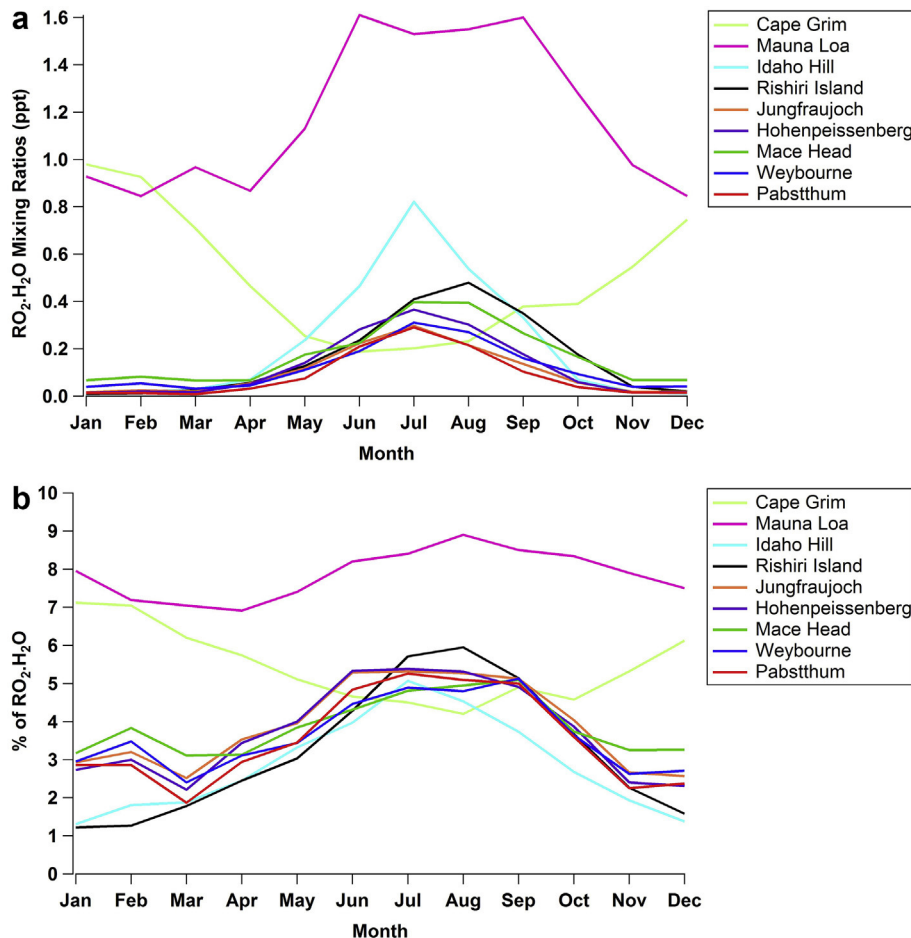


Fig. 5. The seasonal variation of RO₂-H₂O complexation (a) in absolute terms, (b) in percentage of total RO₂ concentration at selected measurement stations.

lower complexation over land (up to 15%) (Fig. 7b). The two competing factors—either water vapour abundance or temperature, exert a large influence on the extent of peroxy radical-water complexation.

The presence of RO₂-H₂O has been examined at higher tropospheric altitudes using the temperature dependence equation (2) of the RO₂-H₂O complex. The percentage concentration of RO₂-H₂O in all 9 vertical levels of the STOCHEM-CRI model was determined at three measurement stations covering various latitudes (e.g. Mace Head in Northern Hemisphere, Cape Grim in Southern Hemisphere, and Mauna Loa in Tropics) and displayed in Fig. 8.

Mauna Loa retains relatively steady levels of complexation due to elevated water vapour concentrations throughout the troposphere. At this site, the degree of the complexation decreases sharply from approximately 1.5 km because of the relatively higher model temperature (283 K) than the other two sites (269 K at Mace Head and 276 K at Cape Grim). The lowest degree of complexation (5%) was observed at approximately 5 km and then the complexation increased steadily up to 14 km because the model temperature is decreasing significantly (dropping to 209 K). In Northern and Southern Hemisphere locations, where the annual variation in water vapour and temperature are more substantial, complexation reduction with each vertical level is a more gradual process (Fig. 8). Although the concentration of RO₂-H₂O is higher in each vertical level of the troposphere in Cape Grim compared with Mace Head, the degree of complexation is found to be lower at Cape Grim because of higher temperatures encountered. The largest fraction of

model RO₂-H₂O complex exists at above Mace Head (17% Northern Hemisphere), at above Cape Grim (14% Southern Hemisphere), and at above Mauna Loa (8% Tropic) at approximately 8 km in the model but in absolute terms the highest mixing ratios are 0.82, 1.34, and 2.25 ppt at the surface level for Mace Head, Cape Grim, and Mauna Loa, respectively. The results suggest that the extent of complexation is a balance between the availability of water content at higher temperature and the favourably of the complex formation at lower temperature.

The existence of RO₂-H₂O could effect RO₂ kinetics in the atmosphere. The formation of the complexes with H₂O may reduce the energy barrier of the transition state of RO₂ reactions with NO, HO₂ or other RO₂ and thereby the reaction rates of these reactions can be enhanced in the presence of H₂O. These new reaction channels could have an effect on the tropospheric production of HO_x, NO_x, O₃, ROOH, and organic nitrates species and have potential importance for the understanding of atmospheric oxidative pathways especially in the marine boundary layer, where RO₂-H₂O complexes are likely to be formed. The rate enhancement would increase the competition between the loss processes (e.g. RO₂ removal by HO₂/RO₂ versus RO₂ removal by NO). The loss of RO₂ by NO is very important in atmospheric chemistry because of direct formation of organic nitrates (RONO₂) or the production of O₃ (through photolysis of NO₂ and further reaction of the formed O-atoms with O₂) in the troposphere. Because of the smaller binding energy, the participation of CH₃O₂-H₂O complex in the peroxy self-reaction is not favoured (English et al., 2008). However, the RO₂

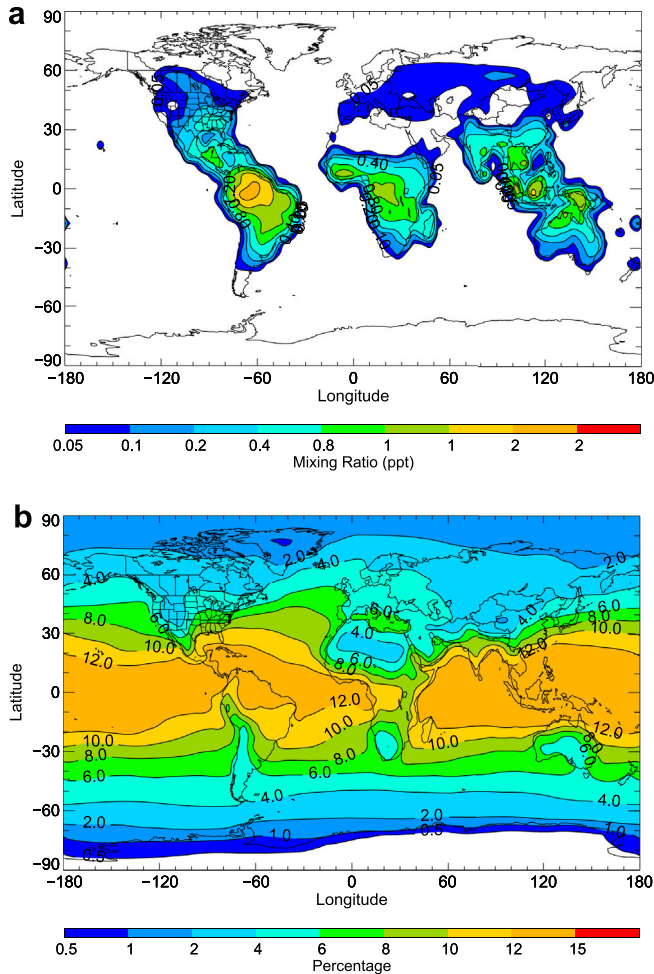


Fig. 6. Annual mean surface level distribution of $C_5H_8O_2 \cdot H_2O$ complexes (using the equilibrium constant of $2.6 \times 10^{-19} \text{ cm}^3 \text{ molecule}^{-1}$) simulated by the STOCHEM-CRI, (a) mixing ratio of $C_5H_8O_2 \cdot H_2O$, (b) percentage of $C_5H_8O_2 \cdot H_2O$ complex formation with respect to $C_5H_8O_2$.

species including $C=O$ or $-OH$ moiety has relatively higher binding energies (Clark et al., 2008) which could enhance the $RO_2 \cdot H_2O$ self-reaction and cross-reaction ($RO_2 \cdot H_2O + HO_2/RO_2$) rate co-efficient. Modest enhancements in rate coefficient would not be so important of course but a significant increase (e.g. a factor of 2) in any of the rate coefficients with NO, HO_2 or other RO_2 with the water complexed RO_2 species or a change in dominant product channels could be important. The significance of the $RO_2 \cdot H_2O$ complexation can be assessed by calculating the enhanced loss of RO_2 through the reaction with NO or through peroxy radical cross reactions due to the existence of $RO_2 \cdot H_2O$ in the troposphere. Considering the increased rate coefficient (a factor of 2), the complexation will enhance the production of O_3 , organic nitrates ($RONO_2$), organic hydroperoxides ($ROOH$) in the lower troposphere by 12% (land) to 14% (ocean). It is of course not possible to speculate further without experimental and/or theoretical studies to fill in the gaps in our knowledge with respect to rate coefficient enhancements and product channels. However, this study suggests that such experimental measurements on the kinetics and products of the reaction between $RO_2 \cdot H_2O$ and NO, RO_2/HO_2 are worthy of investigation.

4. Conclusion

A global 3-D model (STOCHEM-CRI) was used to investigate the

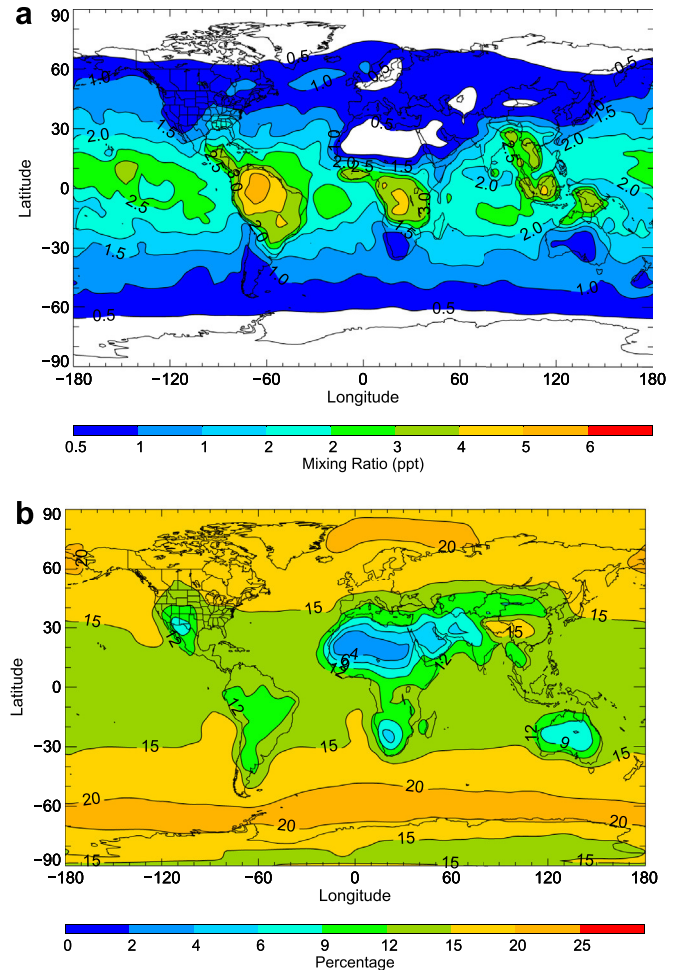


Fig. 7. Annual mean surface level distribution of $RO_2 \cdot H_2O$ complexes (using the temperature dependent equation of the equilibrium constant (Eq. (2)) for $RO_2 \cdot H_2O$) simulated by the STOCHEM-CRI, (a) mixing ratio of $RO_2 \cdot H_2O$, (b) percentage of $RO_2 \cdot H_2O$ complex formation with respect to RO_2 .

distribution of peroxy radicals throughout the lower troposphere. Various datasets acquired from field campaigns were used to evaluate the accuracy of the chemical scheme and dynamical core that characterise the STOCHEM-CRI model. Good agreement between model and measurement data was found for most of the stations, but the low resolution of the model computed average concentrations over each grid square of dimensions 5° latitude $\times 5^\circ$ longitude resulted in an under-prediction of model RO_2 for some stations in relation to the levels recorded in field campaigns. The peak model RO_2 is found in tropics because of higher emissions of VOCs and rapid photochemistry. Both Northern and Southern Hemisphere locations exhibited maximum peroxy radical concentrations in the summer months when O_3 photolysis is at its highest and a minimum in winter when solar intensity is negligible. The presence of $RO_2 \cdot H_2O$ complexes has been found substantially in tropical locations at 300 K where atmospheric moisture is in a high abundance—approaching 10–12% of total peroxy radical concentrations. The biogenically derived isoprene species- H_2O complexes could have a significant impact on the chemistry of their uncomplexed counterparts in the troposphere. Complexation appears to play a more significant role in the upper troposphere at sub ambient temperature. Although the level of complexation is modest, it is not certain what significant effects such complexation will have on reaction rates and product branching ratios.

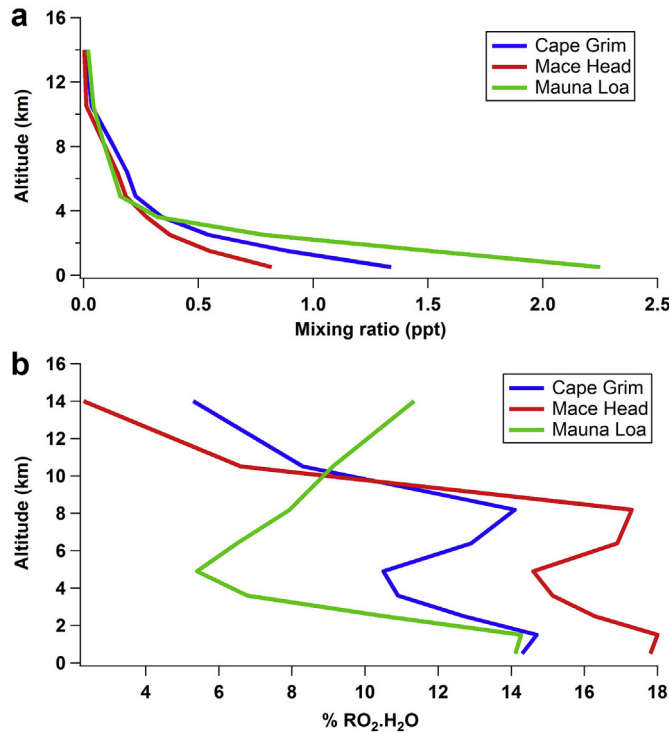


Fig. 8. The proportion of $\text{RO}_2\text{H}_2\text{O}$ in each of the 9 vertical levels of the STOCHEM model, recorded at three measurement stations, (a) in absolute terms, (b) in percentage of total RO_2 concentration.

Acknowledgement

ATA thanks GWR and the U.K. Met. Office for funding (studentship), MCC thanks EPSRC for a studentship, DES and CJP thank NERC and Bristol ChemLabS under whose auspices various aspects of this work was funded.

Appendix A. Supplementary data

Supplementary data related to this article can be found at <http://dx.doi.org/10.1016/j.atmosenv.2015.02.020>.

References

- Aloisio, S., Francisco, J.S., 1998. Existence of a hydroperoxy and water ($\text{HO}_2\text{H}_2\text{O}$) radical complex. *J. Phys. Chem. A* 102, 1899–1902.
- Aloisio, S., Francisco, J.S., Friedl, R.R., 2000. Experimental evidence for the existence of the $\text{HO}_2\text{H}_2\text{O}$ complex. *J. Phys. Chem. A* 104, 6597–6601.
- Andrés-Hernández, M.D., Kartal, D., Reichert, L., Burrows, J.P., Arnek, J.M., Lichtenstern, M., Stock, P., Schlager, H., 2009. Peroxy radical observations over West Africa during AMMA 2006: photochemical activity in the outflow of convective systems. *Atmos. Chem. Phys.* 9, 3681–3695.
- Andrés-Hernández, M.D., Burkert, J., Reichert, L., Stöbener, D., Meyer-Arnk, J., Burrows, J.P., 2001. Marine boundary layer peroxy radical chemistry during the AEROSOLS99 campaign: measurements and analysis. *J. Geophys. Res.* 106 (D18), 20833–20846.
- Archibald, A.T., Tonokura, K., Kawasaki, M., Percival, C.J., Shallcross, D.E., 2011. On the impact of $\text{HO}_2\text{H}_2\text{O}$ complexes in the marine boundary layer: a possible sink for HO_2 . *Terr. Atmos. Ocean. Sci.* 22 (1), 71–78.
- Bin, Q., ZhuQing, W., Akinori, T., Shiro, H., 2009. Photochemical production of ozone in marine boundary layer in the sea of Japan: results of the Rishiri Fall Experiment campaign. *Sci. China Ser. B Chem.* 52 (12), 2366–2372.
- Burkert, J., Andrés-Hernández, M., Stöbener, D., Burrows, J.P., Weissenmayer, M., Kraus, A., 2001. Peroxy radical and related trace gas measurements in the boundary layer above the Atlantic Ocean. *J. Geophys. Res.* 106 (D6), 5457–5478.
- Burkert, J., Andrés-Hernández, M., Reichert, L., Meyer-Arnk, J., Doddridge, B., Dickerson, R.R., Mühlé, J., Zahn, A., Carsey, T., Burrows, J.P., 2003. Trace gas and radical diurnal behaviour in the marine boundary layer during INDOEX 1999. *J. Geophys. Res.* 108 (D8), 8000.
- Cantrell, C.A., Stedman, D.H., Wendel, G.J., 1984. Measurement of atmospheric peroxy-radicals by chemical amplification. *Anal. Chem.* 56 (8), 1496–1502.
- Cantrell, C.A., Lind, J.A., Shetter, R.E., Calvert, J.G., Goldan, P.D., Kuster, W., Fehsenfeld, F.C., Montzka, S.A., Parrish, D.D., Williams, E.J., Buhr, M.P., Westberg, H.H., Allwine, G., Martin, R., 1992. Peroxy radicals in the ROSE experiment: measurement and theory. *J. Geophys. Res.* 97 (D18), 20671–20686.
- Cantrell, C.A., Shetter, R.E., Calvert, J.G., Parrish, D.D., Fehsenfeld, F.C., Goldan, P.D., Kuster, W., Williams, E.J., Westberg, H.H., Allwine, G., Martin, R., 1993. Peroxy radicals as measured in ROSE and estimated from photostationary state deviations. *J. Geophys. Res.* 98, 18355–18366.
- Cantrell, C.A., Shetter, R.E., Gilpin, T.M., Calvert, J.G., Eisele, F.L., Tanner, D.J., 1996. Peroxy radical concentrations measured and calculated from trace gas measurements in the Mauna Loa Observatory Photochemistry Experiment 2. *J. Geophys. Res.* 101, 14653–14664.
- Cantrell, C.A., Shetter, R.E., Calvert, J.G., Eisele, F.L., Williams, E., Baumann, K., Brune, W.H., Stevens, P.S., Mather, J.H., 1997. Peroxy radicals from photostationary state deviations and steady state calculations during the tropospheric OH Photochemistry Experiment at Idaho Hill, Colorado. *J. Geophys. Res.* 102, 6369–6378.
- Carpenter, L.J., Monks, P.S., Bandy, B.J., Penkett, S.A., Galbally, I.E., Meyer, C.P., 1997. A study of peroxy radicals and ozone photochemistry at coastal sites in the northern and southern hemisphere. *J. Geophys. Res.* 102 (D21), 25417–25427.
- Clark, J., English, A.M., Hansen, J.C., Francisco, J.S., 2008. Computational study on the existence of organic peroxy radical-water complexes ($\text{RO}_2\text{H}_2\text{O}$). *J. Phys. Chem. A* 112, 1587–1595.
- Clark, J., Call, S.T., Austin, D.E., Hansen, J.C., 2010. Computational study of isoprene hydroxyalkyl peroxy radical-water complexes ($\text{C}_5\text{H}_8(\text{OH})\text{O}_2\text{H}_2\text{O}$). *J. Phys. Chem. A* 114, 6534–6541.
- Collins, W.J., Stevenson, D.S., Johnson, C.E., Derwent, R.G., 1997. Tropospheric ozone in a Global-Scale Three-Dimensional Lagrangian Model and its response to NO_x emission controls. *J. Atmos. Chem.* 26 (3), 223–274.
- Collins, W.J., Stevenson, D.S., Johnson, C.E., Derwent, R.G., 1999. Role of convection in determining the budget of odd hydrogen in the upper troposphere. *J. Geophys. Res. Atmos.* 104, 26927–26941.
- Cooke, M.C., 2010. Global Modelling of Atmospheric Trace Gases Using the CRI Mechanism (PhD thesis). University of Bristol, UK.
- Derwent, R.G., Stevenson, D.S., Doherty, R.M., Collins, W.J., Sanderson, M.G., 2008. How is surface ozone in Europe linked to Asian and North American NO_x emissions? *Atmos. Environ.* 42, 7412–7422.
- Duderstadt, K.A., Carroll, M.A., Sillmant, S., Wang, T., Albercoot, G.M., Fengt, L., Parrish, D.D., Holloway, J.S., Fehsenfeld, F.C., Blakes, D.R., Blakes, N.J., Forbe, G., 1998. Photochemical production and loss rates of ozone at Sable Island, Nova Scotia during the North Atlantic Regional Experiment (NARE) 1993 summer intensive. *J. Geophys. Res.* 103, 13531–13555.
- English, A.M., Hansen, J.C., Szente, J.J., Maricq, M.M., 2008. The effects of water vapour on the CH_3O_2 self-reaction and reaction with HO_2 . *J. Phys. Chem. A* 112, 9220–9228.
- Fleming, Z.L., Monks, P.S., Rickard, A.R., Heard, D.E., Bloss, W.J., Seakins, P.W., Still, T.J., Sommariva, R., Pilling, M.J., Morgan, R., Green, T.J., Brough, N., Mills, G.P., Penkett, S.A., Lewis, A.C., Lee, J.D., Saiz-Lopez, A., Plane, J.M.C., 2006a. Peroxy radical chemistry and the control of ozone photochemistry at Mace Head, Ireland during summer of 2002. *Atmos. Chem. Phys.* 6, 2193–2214.
- Fleming, Z.L., Monks, P.S., Rickard, A.R., Bandy, B.J., Brough, N., Green, T.J., Reeves, C.E., Penkett, S.A., 2006b. Seasonal dependence of peroxy radical concentrations at a Northern hemisphere marine boundary layer site during summer and winter: evidence for radical activity in winter. *Atmos. Chem. Phys.* 6, 5415–5433.
- Fuchs, H., Brauers, T., Häseler, R., Holland, F., Mihelcic, D., Müsgen, P., Rohrer, F., Wegener, R., Hofzumahaus, A., 2009. Intercomparison of peroxy radical measurements obtained at atmospheric conditions by laser-induced fluorescence and electron spin resonance spectroscopy. *Atmos. Meas. Tech.* 2, 55–64.
- Geyer, A., Bächmann, K., Hofzumahaus, A., Holland, F., Konrad, S., Klüpfel, T., Pätz, H.W., Perner, D., Mihelcic, D., Schäfer, H.J., Volz-Thomas, A., Platt, U., 2003. Nighttime formation of peroxy and hydroxyl radicals during the BERLIOZ campaign: observations and modelling studies. *J. Geophys. Res.* 108, 8249.
- Granier, C., Lamarque, J.F., Mieville, A., Muller, J.F., Olivier, J., Orlando, J., Peters, J., Petron, G., Tyndall, S., Wallens, S., 2005. POET, A Database of Surface Emissions of Ozone Precursors. <http://www.aerojussieu.fr/project/ACCENT/POET.php>.
- Green, T.J., Reeves, C.E., Brough, N., Edwards, G.D., Monks, P.S., Penkett, S.A., 2003. Airborne measurements of peroxy radicals using the PERCA technique. *J. Environ. Monit.* 5, 75–83.
- Handsides, G.M., Plass-Dülmer, C., Gilge, S., Bingemer, H., Berresheim, H., 2003. Hohenpeissenberg Photochemical Experiment (HOPE 2000): measurements and photostationary state calculations of OH and peroxy radicals. *Atmos. Chem. Phys.* 3, 1565–1588.
- Hanke, M., Uecker, J., Reiner, T., Arnold, F., 2002. Atmospheric peroxy radicals: ROXMAS, a new mass-spectrometric methodology for speciated measurements of HO_2 and $\sum\text{RO}_2$ and first results. *Int. J. Mass Spectrom.* 213 (2–3), 91–99.
- Heard, D.E., Pilling, M.J., 2003. Measurement of OH and HO_2 in the troposphere. *Chem. Rev.* 103, 5163–5198.
- Jaffe, D., Mahura, A., Kelley, J., Atkins, J., Novelli, P.C., Merrill, J., 1997. Impact of Asian emissions on the remote North Pacific atmosphere: interpretation of CO data from Shemya, Guam, Midway and Mauna Loa. *J. Geophys. Res.* 102 (D23), 28627–28635.
- Jenkin, M.E., Clemithshaw, K.C., 2000. Ozone and other secondary photochemical

- pollutants: chemical processes governing their formation in the planetary boundary layer. *Atmos. Environ.* 34, 2499–2527.
- Jenkin, M.E., Watson, L.A., Utembe, S.R., Shallcross, D.E., 2008. A Common Representative Intermediate (CRI) mechanism for VOC degradation. Part-1: gas phase mechanism development. *Atmos. Environ.* 42, 7185–7195.
- Jimi, S.I., Gras, J.L., Siems, S.T., Krummel, P.B., 2007. A short climatology of nanoparticles at the cape grim baseline air pollution station, Tasmania. *Environ. Chem.* 4, 301–309.
- Johnson, C.E., Stevenson, D.S., Collins, W.J., Derwent, R.G., 2002. Interannual variability in methane growth rate simulated with a coupled ocean-atmosphere-chemistry model. *Geophys. Res. Lett.* 29, 1903.
- Kaiser, A., Scheifinger, H., Spangl, W., Weiss, A., Gilge, S., Fricke, W., Ries, L., Cemas, D., Jesenovec, B., 2007. Transport of nitrogen oxides, carbon monoxide and ozone to the Alpine global atmosphere Watch stations jungfraujoch (Switzerland), Zugspitze and hohenpeissenberg (Germany), Sonnblick (Austria) and Mt. Krvavec (Slovenia). *Atmos. Environ.* 41, 9273–9287.
- Kanno, N., Tonokura, K., Koshi, M., 2006. Equilibrium constant of the HO₂–H₂O complex formation and kinetics of HO₂+HO₂-H₂O: implications for tropospheric chemistry. *J. Geophys. Res.* 111, D20312.
- Kukui, A., Aucellet, G., Le Bras, G., 2008. Chemical ionisation mass spectrometer for measurements of OH and peroxy radical concentrations in moderately polluted atmospheres. *J. Atmos. Chem.* 61, 133–154.
- LaFranchi, B.W., Wolfe, G.M., Thornton, J.A., Harrold, S.A., Browne, E.C., Min, K.E., Wooldridge, P.J., Gilman, J.B., Kuster, W.C., Goldan, P.D., de Gouw, J.A., McKay, M., Goldstein, A.H., Ren, X., Mao, J., Cohen, R.C., 2009. Closing the peroxy acetyl nitrate budget: observations of acyl peroxy nitrates (PAN, PPN, and MPAN) during BEARPEX 2007. *Atmos. Chem. Phys.* 9, 7623.
- Lightfoot, P.D., Cox, R.A., Crowley, J.N., Destriau, M., Hayman, G.D., Jenkin, M.E., Moortgat, G.K., Zabel, F., 1992. Organic peroxy radicals: kinetics, spectroscopy and tropospheric chemistry. *Atmos. Environ.* 26, 1805–1961.
- Liu, Y., Morales-Cueto, R., Hargrove, J., Medina, D., Zhang, J., 2009. Measurements of peroxy radicals using chemical amplification-Cavity Ringdown Spectroscopy. *Environ. Sci. Technol.* 43, 7791–7796.
- Madronich, S., Calvert, J.G., 1990. Permutation reactions of organic peroxy radicals in the troposphere. *J. Geophys. Res.* 95 (D5), 5697–5715.
- Mihelcic, D., Holland, F., Hofzumahaus, A., Hoppe, L., Konrad, S., Müsgen, P., Pätz, H.-W., Schäfer, H.-J., Schmitz, T., Volz-Thomas, A., Bächmann, K., Schlomski, S., Platt, U., Geyer, A., Aliche, B., Moortgat, G.K., 2003. Peroxy radicals during BERLIOZ at Pabstthum: measurements, radical budgets and ozone production. *J. Geophys. Res.* 108 (D4), 8254.
- Monks, P.S., 2005. Gas-phase radical chemistry in the troposphere. *Chem. Soc. Rev.* 34, 376–395.
- Monks, S.M., Carpenter, L.J., Penkett, S.A., Ayers, G.P., Gillet, R.W., Galbally, I.E., Meyer, C.P., 1998. Fundamental ozone photochemistry in the remote MBL: the SOAPEX experiment, measurement and theory. *Atmos. Environ.* 32, 3647–3664.
- Sander, S.P., Friedl, R.R., Barker, J.R., Golden, D.M., Kurylo, M.J., Wine, P.H., Abbatt, J.P.D., Burkholder, J.B., Kolb, C.E., Moortgat, G.K., Huie, R.E., Orkin, V.L., 2011. Chemical Kinetics and Photochemical Data for Use in Atmospheric Studies. Evaluation Number 17, JPL Publication 10-6. Jet Propulsion Laboratory, Pasadena, CA.
- Sanderson, M.G., Collins, W.J., Derwent, R.G., Johnson, C.E., 2003. Simulation of global hydrogen levels using a Lagrangian three-dimensional model. *J. Atmos. Chem.* 46 (1), 15–28.
- Thompson, A.M., 1992. The oxidizing capacity of the earth's atmosphere: probable past and future changes. *Science* 256, 1157–1165.
- Tyndall, G.S., Cox, R.A., Granier, C., Lesclaux, R., Moortgat, G.K., Pilling, M.J., Ravishankara, A.R., Wallington, T.J., 2001. Atmospheric chemistry of small organic peroxy radicals. *J. Geophys. Res.* 106, 12157–12182.
- Utembe, S.R., Watson, L.A., Shallcross, D.E., Jenkin, M.E., 2009. A Common Representative Intermediates (CRI) mechanism for VOC degradation. Part 3: development of a secondary organic aerosol module. *Atmos. Environ.* 43, 1982–1990.
- Utembe, S.R., Cooke, M.C., Archibald, A.T., Jenkin, M.E., Derwent, R.G., Shallcross, D.E., 2010. Using a reduced Common Representative Intermediates (CRI v2-R5) mechanism to simulate tropospheric ozone in a 3-D Lagrangian chemistry transport model. *Atmos. Environ.* 13, 1609–1622.
- Utembe, S.R., Cooke, M.C., Archibald, A.T., Shallcross, D.E., Derwent, R.G., Jenkin, M.E., 2011. Simulating secondary organic aerosol in a 3-D Lagrangian chemistry transport model using the reduced Common Representative Intermediate mechanism (CRI v2-R5). *Atmos. Environ.* 45, 1604–1614.
- Watson, L.A., Shallcross, D.E., Utembe, S.R., Jenkin, M.E., 2008. A Common Representative Intermediate (CRI) mechanism for VOC degradation. Part 2: gas phase mechanism reduction. *Atmos. Environ.* 42 (31), 7196–7204.
- Wallington, T.J., Dagaut, P., Kurylo, M.J., 1992. Ultraviolet absorption cross-sections and reaction kinetics and mechanisms for peroxy radicals in the gas-phase. *Chem. Rev.* 92 (4), 667–710.
- Zanis, P., Monks, P.S., Schuepbach, E., Penkett, S.A., 1999. On the relationship of HO₂+RO₂ with j(O¹D) during the Free Tropospheric Experiment (FREETEX'96) at the Jungfraujoch Observatory (3580 m above sea level) in the Swiss Alps. *J. Geophys. Res.* 104 (D21), 26913–26925.